Mine Water Environ (2015) 34:213–222
DOI 10.1007/s10230-014-0309-1

TECHNICAL ARTICLE

Lepidocrocite Formation Kinetics from Schwertmannite in Fe(II)-Rich Anoxic Alkaline Medium

Susanta Paikaray · Stefan Peiffer

Received: 29 January 2014 / Accepted: 11 September 2014 / Published online: 23 September 2014

Abstract Effect of dissolved ferrous iron [$Fe(II)_{aq}$ = 0–1.0 mM] on stability of schwertmannite containing ≈40 wt% Fe(III) and 15 wt% SO_4^{2-} [with and without 0.92 wt% sorbed As(III)] was investigated in anoxic alkaline conditions at pH 8 for 154 h. New product formation, sulfate, iron, and arsenic release kinetics were examined using diffractogram, microscopic, spectroscopic and geochemical techniques. Both schwertmannite types were incompletely transformed to lepidocrocite with a platy tabular morphometry. Product formation was accelerated with increased $Fe(II)_{aq}$, while sorbed As(III) markedly hindered lepidocrocite formation. Almost 50–57 % of the SO_4^{2-} was released from schwertmannite within 154 h in the absence of $Fe(II)_{aq}$, while its presence inhibited its release. Some of the sorbed As(III) was released during lepidocrocite formation with a maximum in the presence of 1.0 mM $Fe(II)_{aq}$ (0.02 %, 21 μg L^{-1}), presumably due to catalytic action of $Fe(II)_{aq}$ on schwertmannite dissolution, which likely re-precipitated as lepidocrocite with considerable surface-adsorbed SO_4^{2-}.

Keywords Acid mine drainage · As(III) mobilization · Fe(II) catalysis · Fe(II)–Fe(III) electron transfer · Lepidocrocite formation · Schwertmannite metastability · Sulfate desorption

S. Paikaray · S. Peiffer
Department of Hydrology, University of Bayreuth, 95440 Bayreuth, Germany

S. Paikaray (✉) · S. Peiffer
Department of Earth and Environmental Sciences, Indian Institute of Science Education and Research Bhopal, Bhopal, India
e-mail: susanta.paikaray@gmail.com

Introduction

Iron (hydr)oxides precipitated in and near mine tailings play an important role in acid mine drainage (AMD) affected soil and water quality by acting as potential natural sinks because of their high retentive capacity for trace metals (Carlson et al. 2002; Courtin-Normade et al. 2005; Fukushi et al. 2003; Webster et al. 1998; Winland et al. 1991). The amorphous or poorly crystalline minerals, e.g. schwertmannite (STM), are the earliest formed precipitates and are subsequently transformed to more crystalline forms, such as goethite (Gt), via dissolution-reprecipitation and solid-state transformation. This ultimately leads to co-occurrence of these phases in most AMD localities (Acero et al. 2006; Davidson et al. 2008; Jönsson et al. 2005; Regenspurg et al. 2004).

Schwertmannite (ideally $Fe_8O_8(OH)_6SO_4$), the brownish-yellow, poorly crystalline Fe(III)-oxyhydroxy sulfate precipitate that structurally resembles akaganéite, is stable in a narrow pH range between 3.0 and 4.5 (Bigham et al. 1990, 1996). Its stability when exposed to alkaline environments draws special research attention (Collins et al. 2010; Johnston et al. 2011; Jönsson et al. 2005; Regenspurg et al. 2004; Wang et al. 2006) because it is a better trace metal scavenger than its more crystalline counterparts (Paikaray et al. 2014). STM transformation kinetics in oxic conditions has demonstrated that pH is the critical controlling parameter, with elevated pH conditions accelerating STM dissolution and Gt formation (Eq. 1) (Acero et al. 2006; Jönsson et al. 2005; Kumpulainen et al. 2008; Paikaray and Peiffer 2012; Schwertmann and Carlson 2005). Hematite forms at high temperatures (>600 °C; Henderson and Sullivan 2010), but, its formation rates in oxic and even alkaline pH conditions is extremely slow, taking a few months or even a year for complete formation (Jönsson

et al. 2005; Knorr and Blodau 2007; Kumpulainen et al. 2008; Paikaray and Peiffer 2012; Regenspurg et al. 2004); the presence of anions or trace metals further retards the rate marginally (Acero et al. 2006; Jönsson et al. 2005; Paikaray and Peiffer 2012; Regenspurg et al. 2004; Schroth and Parnell 2005).

$$Fe_8O_8(OH)_x(SO_4)_y + 2xH_2O \rightarrow 8FeOOH + ySO_4^{2-} + 2xH^+, \quad \text{where} \quad x = 8 - 2y,\ 1 < y < 1.75 \tag{1}$$

Fe-respiring bacteria add continuous flux of Fe(II) into most AMD-affected areas. Bacterial Fe(III)-reduction processes are coupled with generation of alkalinity, hence driving conditions away from the STM stability window (pH 3.0–4.5, Bigham et al. 1990, 1996). Burton et al. (2008) demonstrated complete STM transformation to Gt in the presence of 1–10 mM $Fe(II)_{aq}$ at pH >5.5, where the rates were controlled by increasing $Fe(II)_{aq}$. Similar observations have also been reported in coastal low lands in Eastern Australia (Burton et al. 2007, 2008), with formation of iron sulfide minerals like mackinawite. However, the effect of $Fe(II)_{aq}$ below 1 mM is still unclear.

The precipitated STM in such localities are often rich in As(III)/As(V) due to STM's high sorptive affinity, which in turn is due to STM's high surface area (>200 $m^2\ g^{-1}$), exchangeable SO_4^{2-} ($\approx$35 %), and poor crystalline nature (Egal et al. 2009; Morin et al. 2003; Webster et al. 1998). This is important since the mobility of sorbed arsenic can adversely influence mine water geochemistry. For example, high As enrichment in Bangladesh groundwater, which seriously affects $\approx$70 million people, is believed to be caused by reductive dissolution of iron oxides in alkaline conditions (McArthur et al. 2001). Fukushi et al. (2003) and Regenspurg et al. (2004) demonstrated how the presence of dissolved As can enhance STM stability against mineralogical transformation, where slow oxic transformations cause negligible As release (<1 %, Acero et al. 2006), and how As can be totally re-adsorbed onto STM (Paikaray and Peiffer 2012). On the other hand, research on such aspects during rapid transformation in $Fe(II)_{aq}$-enriched environments is rare. Burton et al. (2010) demonstrated hindrance of transformation rates and product formation by adsorbed As(III). Their study, however, maintained a constant pH of 6.5 and $Fe(II)_{aq}$ (10 mM), with 1 mM of As(III) present in the aqueous phase, and concluded that Gt formed after 9 days of ageing (Burton et al. 2010). The catalytic effect of $Fe(II)_{aq}$ on prior As(III)-sorbed STM metastability needs to be addressed. The present research investigated how trace amounts of dissolved Fe(II) ($\leq$1.0 mM) affects STM metastability in an alkaline (pH 8.0) medium, and its consequential influence on aqueous geochemistry.

Materials and Methods

Schwertmannite Samples

Two STM types, with (SHM-As) and without (SHM) sorbed As(III), were used in this study. SHM was synthesized through bacterial oxidation of Fe(II) from SO_4^{2-}-rich aqueous phase at GEOS, Freiberg, Germany between pH 2.9 and 3.2 (Glombitza et al. 2007). The brownish yellow precipitates were air dried at room temperature (RT, 22–25 °C) after synthesis and the sieved particles (<63 μm) were used without further treatment. As(III) was loaded (100 mg L^{-1}) onto part of the SHM in oxic conditions during 5 days batch equilibrium studies at pH 3.0 using 10 g L^{-1} sediment load. The solid phase was separated by centrifugation at 4,500 rpm for 15 min (Centrikon T-42 K, ALC International Srl. Italy), oven dried ($\approx$30 °C), and stored at RT. Mass balance calculations yielded 0.92 wt% As(III) loading in the solid phase; extended X-ray absorption near-edge structure (XANES) spectroscopic investigation showed no As(III) surface oxidation to As(V) (±5 % instrumental error) (Paikaray et al. 2011, 2012).

Transformation Experiments

The glass serum reactor vials were conditioned in 10 % (v/v) HNO_3 overnight and then rinsed with milli-Q H_2O several times before starting the transformation. All chemicals were of analytical grade and most solutions were prepared fresh when required, using ultrapure N_2 (95 % N_2 + 5 % H_2) purged milli-Q H_2O, which had been purged for at least 2 h to ensure complete deoxygenation. A glove box was conditioned for 15 days prior to starting the ageing experiments by purging 3–4 times daily with ultrapure N_2 gas and then was regularly purged 3 times during the ageing experiments.

Ageing experiments were conducted at pH 8.0 for 154 h using 0.25 g of SHM and SHM-As in 25 mL O_2-free milli-Q H_2O in the presence of 0, 0.4, 0.7, and 1.0 mM $Fe(II)_{aq}$. Appropriate quantities of $FeCl_2$ stock solutions (0.1 M) and 2-(4-(2-hydroxyethyl)-1-piperazinyl)-ethanesulphonic acid sodium salt (HEPES-Na, $pK_a = 7.66$) buffer was used to adjust the $Fe(II)_{aq}$ and pH before adding the solid phase. As equilibration of STM with aqueous phase requires several days (Paikaray and Peiffer 2010) and is susceptible to mineralogical changes at such high pH conditions, the ageing experiments were investigated without pre-equilibration. The reactor vials were sealed immediately and tumbled in an overhead shaker. A pair of the reactor vials was collected at regular intervals, the aqueous phase was separated by filtration (0.45 μm ROTH filter), and the solid phase was air dried inside the glove box.

Analytical Methods

Mineralogical investigations were carried out using a SIEMENS D5000 X-ray diffractometer with a Co–K_α radiation source. The samples were scanned four times between 10 and 80° 2θ using 0.20° 2θ step size and 15 s count time; the averaged diffractograms are presented here. Surface functional groups were examined by Fourier transform infrared (FTIR, Vector 22, Bruker Optik GmbH, Ettingen, Germany) spectroscopic technique using OPUS-NT software. Pellets were prepared by homogenous mixing of 2 mg of sample with 200 mg of KBr at ≈8 kbar pressure and scanned between 350 and 4,500 cm^{-1} with 1 cm^{-1} resolution. A total of 32 scans were collected for each measurement in transmission mode; the background spectra were subtracted automatically by background scans before running the samples. Scanning electron microscopic (SEM) study was carried out using a LEO 1,530 equipped with a Shotky cathode and GEMINI column with ZrO_2 radiation source (ZEISS, Germany). The powdered samples were mounted on a carbon tape, which were sputtered in a Cressington sputter coater 208 HR with 1.3 nm Platin (≈1 min, 40 mA) and imaged at 3 kV. The specific surface area (SSA) was determined by a five point N_2 point adsorption isotherm (BET) method (Gemini 2375 v 5.01).

Iron and SO_4^{2-} were measured spectrophotometrically (Cary 1E, Varian Analytical Instruments, Darmstadt, Germany) at 512 and 420 nm wavelength using the 1,10-phenanthrolene (Tamura et al. 1974) and $BaCl_2$–gelatin (Tabatabai 1974) method, respectively. The pH was measured using a Mettler Toledo Inlab 420 electrode, calibrated using pH 4.0 and 7.0 buffers. Arsenic was determined by atomic absorption spectrophotometetry (AAS) equipped with a graphite furnace (AAS ZEEnit 60, Analytik Jena AG, Jena, Germany) at 193.7 nm.

Results and Discussions

Characterization of Schwertmannites

The poor crystalline nature of both specimens (SHM and SHM-As) can be inferred from the general broad XRD patterns (Fig. 1a) with the three common SO_4^{2-} IR absorption bands typical of STM, at 1,120 cm^{-1}: $\nu_3(SO_4)$; 981 cm^{-1}: $\nu_1(SO_4)$, and; 610 cm^{-1}: $\nu_4(SO_4)$, Fig. 1b (Bigham et al. 1990; Boily et al. 2010). The appearance of the low intensity IR band at ≈1,385 cm^{-1} and overall morphological degradation of the SHM-As (Fig. 1d) is believed to be due to As(III) retention (Paikaray et al. 2011, 2012). Sorbed As(III) (0.92 wt%) caused a slight increase in SSA from 14.7 (SHM) to 17.1 (SHM-As) $m^2\ g^{-1}$ (Table 1). This represents slight differences in properties between the two specimens before ageing. Elemental analysis yielded $Fe_8O_8(OH)_{4.64}\ (SO_4)_{1.68}$ and $Fe_8O_8(OH)_{4.82}\ (SO_4)_{1.59}$ as the chemical formula for SHM and SHM-As, respectively.

Product Formation

The diffractograms of the transformed products after 5, 10, 58, 106, and 154 h for SHM and only 58, 106, and 154 h for SHM-As (no changes <58 h) are shown in Fig. 2 and Fig. 3, respectively. Typical schwertmannite diffractogram peaks at 0.152, 0.168, 0.191, 0.230, 0.254, and 0.330 nm were seen in all the samples, even after 154 h, in the presence of 1.0 mM $Fe(II)_{aq}$, showing the continued existence of STM in the final transformed phase. Broad XRD peaks were noticed at 0 and 0.4 mM $Fe(II)_{aq}$ until 154 h ageing, with a slight sharpening indicating that STM crystallization increased as $Fe(II)_{aq}$ was increased to 0.7 and 1.0 mM. In the case of SHM, lepidocrocite (Lp) appeared together with STM after 106 h in the presence of 0.7 and 1.0 mM $Fe(II)_{aq}$ until 154 h of ageing (0.626, 0.329, and 0.247 nm d-spacing). In the case of SHM-As, although most of the STM peaks were diminished, except at 0.254 nm in the presence of 0.7 mM $Fe(II)_{aq}$, traces of Lp were visible in the presence of 1.0 mM $Fe(II)_{aq}$ after 106 h, indicating slow transformation rates due to sorbed As(III). However, the appearance of Lp diffractograms in both specimens occurred together with STM and did not show XRD evidence of complete transformation to Lp, even after 154 h in the presence of up to 1.0 mM $Fe(II)_{aq}$.

Splitting of the 1,120 cm^{-1} $\nu_3(SO_4)$ peak and the appearance of a 1,050 cm^{-1} peak and a low intensity 1,022 cm^{-1} IR band (Fig. 4) further indicated formation of new minerals, with the latter low-intensity peak indicating Lp formation (Cornell and Schwertmann 2006; Liu et al. 2007b).

Only morphological degradation of STM was observed from SEM images up to 0.4 mM $Fe(II)_{aq}$, supporting the diffractogram indication of no new mineral formation. Growth of Lp crystals on SHM was observed at 0.7 mM $Fe(II)_{aq}$, while complete morphological decay without any evidence of Lp crystals was observed in the case of SHM-As. On the other hand, well-grown platy Lp crystals (thickness <1 nm, Fig. 5) together with STM were noticed in the presence of 1.0 mM $Fe(II)_{aq}$, with both specimens confirming XRD findings of Lp formation. Nevertheless, the transformation remained incomplete and both Lp and STM were found as the final product after 154 h ageing.

Both the XRD and SEM observations of the transformed products indicate that: (1) STM transformation was accelerated by increased $Fe(II)_{aq}$, possibly through catalytic action, and was strongly dependent on ageing time, (2) sorbed As(III) substantially hindered the Fe(II) catalytic

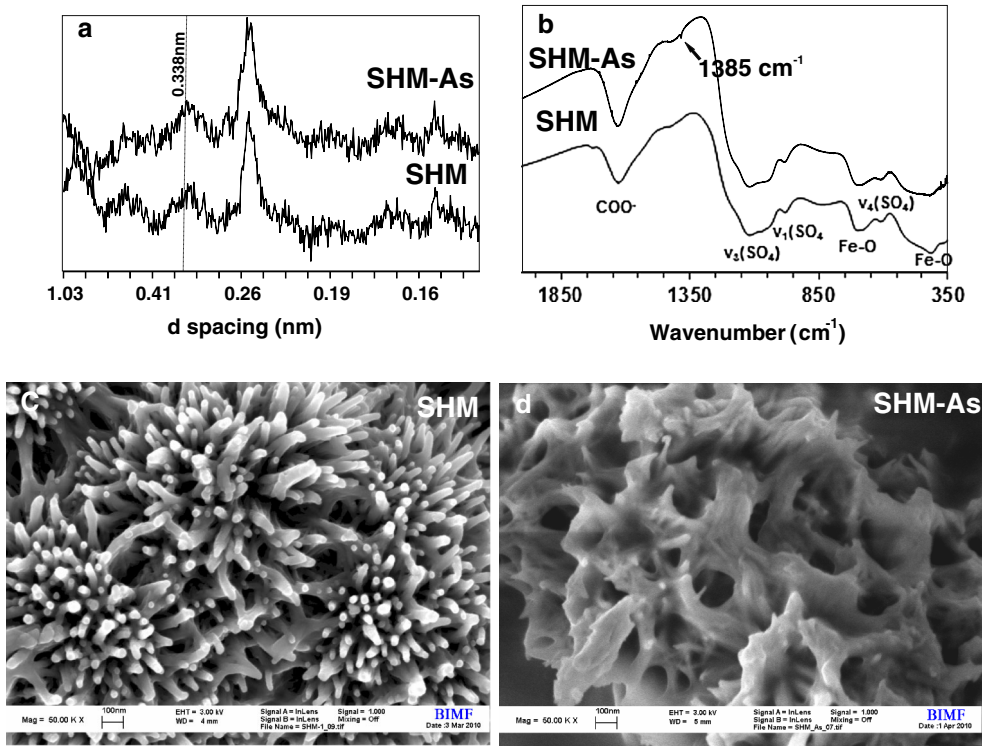

Fig. 1 **a** X-ray diffractograms, **b** FTIR spectra, **c** SEM images of SHM, and **d** SHM-As. The *y-axis* in **a** and **b** are intensity and transmission, respectively. The SHM denotes schwertmannite without adsorbed As(III), while SHM-As denotes schwertmannite adsorbed with 0.92 wt% As(III)

Table 1 Characteristics of Schwertmannites

Samples	SSA (m^2/g)	As(III) (wt%)	Chemical formula
SHM	14.7	0	$Fe_8O_8(OH)_{4.64}(SO_4)_{1.68}$
SHM-As	17.1	0.92	$Fe_8O_8(OH)_{4.82}(SO_4)_{1.59}$

effect on transformation, and (3) STM was transformed to platy Lp incompletely after 154 h of contact with 1.0 mM $Fe(II)_{aq}$ phase, which indicates the requirement of more $Fe(II)_{aq}$ for faster and complete transformation to a crystalline phase. Such an effect was reported by Burton et al. (2007), who found better crystalline Lp and Gt formation as $Fe(II)_{aq}$ concentrations increased to 40 mM. However, those authors found that Gt was the major phase after 24 h ageing, even in the presence of 1.0 mM $Fe(II)_{aq}$ at pH 6.5, which disagrees with the present observations. This could possibly be due to the lower sediment:solution ratio (8 g L^{-1}) in their study, compared to ours (10 g L^{-1}); less mass would have more easily transformed to stable end products. Lepidocrocite (γ-FeOOH) is considered to be an unstable iron oxyhydroxide that finally transforms to Gt or Hm depending on aqueous pH and temperature, but this reaction is reported to be very slow at ambient temperature and neutral pH (Cornell and Schwertmann 2006; Pederson et al. 2005, 2006). The present study demonstrates that Lp can form from STM, at least in the presence of 1.0 mM $Fe(II)_{aq}$. Burton et al. (2010) showed complete transformation of STM to Gt within 9 days of ageing in the presence of 10 mM $Fe(II)_{aq}$ where the presence of sorbed As(III) (≈1.5 wt%, 30–34 % oxidized to As(V)) resulted in incomplete transformation (≈72 % Gt); they did not find evidence of Lp after 9 days, as we found. Their higher $Fe(II)_{aq}$ and elongated ageing period might explain such a complete transformation to the stable mineral phase; Lp might have formed as an intermediate phase and then rapidly transformed to Gt.

Iron and Sulfate Release Kinetics

Neither Fe(II) nor Fe(III) were detected in aqueous phase for either SHM and SHM-As throughout the 154 h ageing period, indicating that either all of the initially used $Fe(II)_{aq}$ (0.4–1.0 mM) was consumed by the STM during transformation or sorbed onto the transformed products, or aqueous Fe(III) from dissolved SHM/SHM-As rapidly reprecipitated prior to the first measurement (after 5 h). Schwertmannite was still found as a major mineral phase after 5 h of ageing. Thus, the complete consumption of $Fe(II)_{aq}$ indicates that the amount that might have been

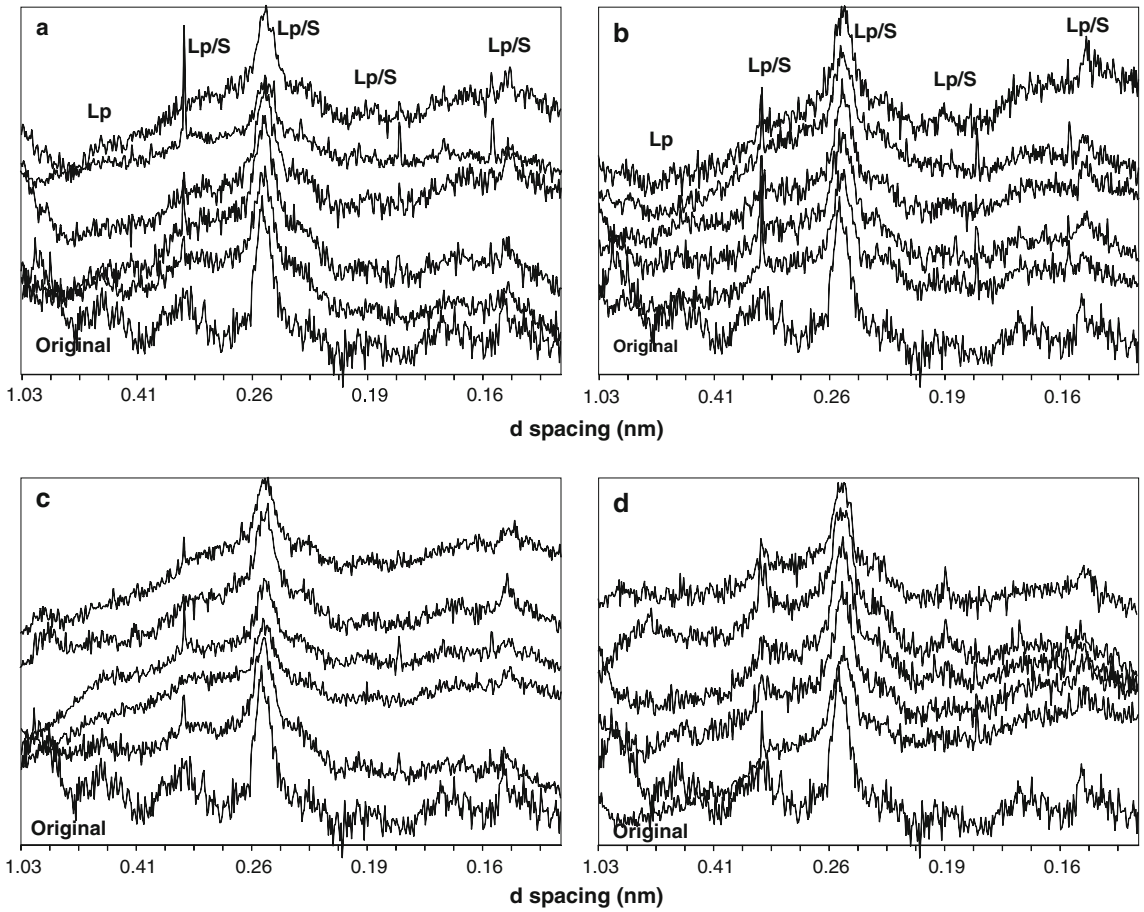

Fig. 2 X-ray diffractograms of transformed products and original (*marked as original*) schwertmannite (SHM) at 0.0 (**a**), 0.4 (**b**), 0.7 (**c**) and 1.0 (**d**) mM $Fe(II)_{aq}$. The diffractograms from *bottom to top* represent transformed products after 5, 10, 58, 106 and 154 h, respectively. The *y-axis* in is intensity. The sharp peak at ≈0.336 nm in few samples, especially in 0 mM $Fe(II)_{aq}$, may be arising because of background noises

adsorbed onto STM possibly triggered its dissolution, resulting in enhanced aqueous SO_4^{2-} (see "Discussion") instead of adsorption onto the transformed product. Liu et al. (2005, 2009), based on a Fe(II) catalytic study on ferrihydrite (Fh) and δ-FeOOH, reported an increase of $Fe(II)_{aq}$ concentrations during the original mineral dissolution. However, their reactions were investigated for only 30 min and $Fe(II)_{aq}$ increased, causing a transformation to Hm as Fe(II) acted as a catalyst for rapid dissolution of Fh and δ-FeOOH.

Similarly, no pH change was observed during any sampling period, in contrast to Burton et al. (2007), indicating that the reactors were well buffered against the large proton release during STM dissolution (Eq. 1) to maintain the pH at 8.0. On the other hand, significant SO_4^{2-} was released from both specimens; maximum release was observed in the absence of $Fe(II)_{aq}$ [≈57 % (SHM) and ≈50 % (SHM-As)] and the least release was observed in the presence of 0.4 mM $Fe(II)_{aq}$ [≈45 % (SHM) and ≈44 % (SHM-As)] after 154 h (Fig. 6a), demonstrating that dissolution of original STM had occurred. Previous researchers have shown that almost 33–35 % SO_4^{2-} adsorbs onto STM surfaces, which can be easily released through dissolution or exchange during sorption processes (Bigham et al. 1990; Jönsson et al. 2005). However, the 50–57 % released fractions in this study clearly indicate release of structural SO_4^{2-} in addition to the surface-adsorbed fractions commonly observed in oxic conditions (Acero et al. 2006; Jönsson et al. 2005; Paikaray and Peiffer 2012; Peretyazhko et al. 2009). The negative influence of $Fe(II)_{aq}$ on SO_4^{2-} release contradicts previous reports by Burton et al. (2010), who reported increased SO_4^{2-} release from 59 to 61 % as $Fe(II)_{aq}$ concentrations increased from 0 to 10 mM during 9 days of anoxic ageing. Those authors conducted their study at a pH of 6.5, which is very close to the STM point of zero charge ($pH_{PZC} = 6.6$, Regenspurg et al. 2004), which might have generated a slightly positive to neutral surface charge that is unsuitable for $FeOH^+$ (dominant Fe(II) species at pH ≈7, Liu et al. 2005, 2009) adsorption on its surface.

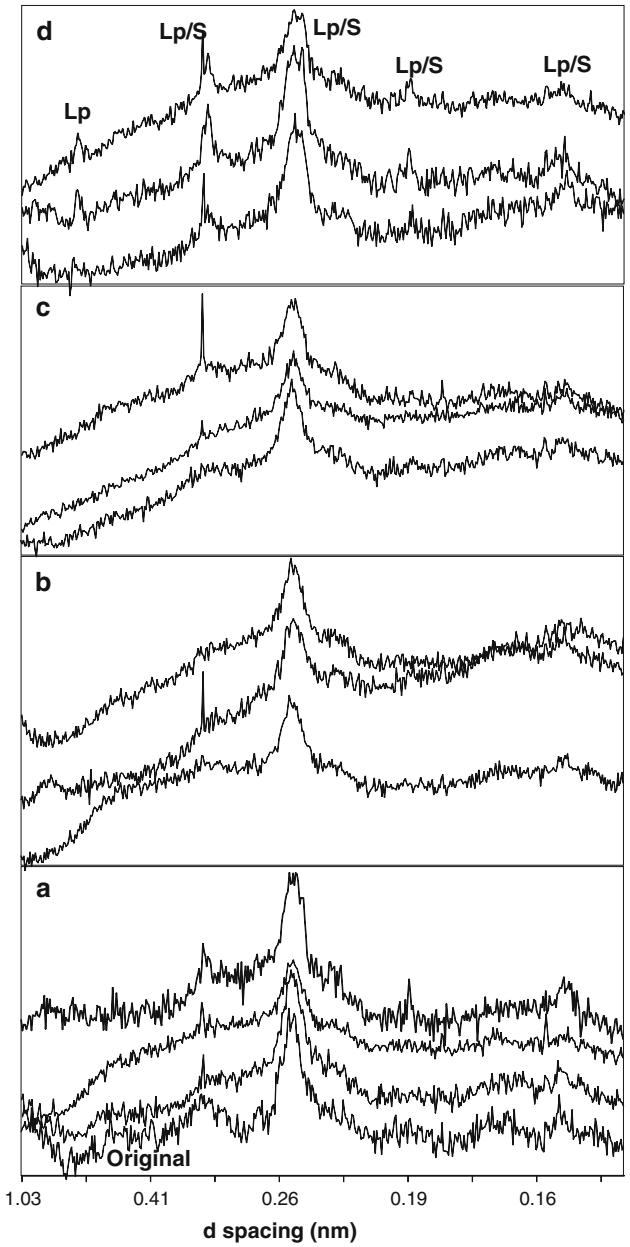

Fig. 3 X-ray diffractograms of transformed products and original, as marked in **a**, of As(III)-loaded schwertmannite (SHM-As) at **a** 0.0, **b** 0.4, **c** 0.7 and **d** 1.0 mM $Fe(II)_{aq}$. The diffractograms from *bottom to top* represent transformed products after 58, 106, and 154 h, respectively. The *y-axis* is intensity. The sharp peak at ≈0.336 nm in a few samples, especially in 0 mM $Fe(II)_{aq}$, may be due background noise

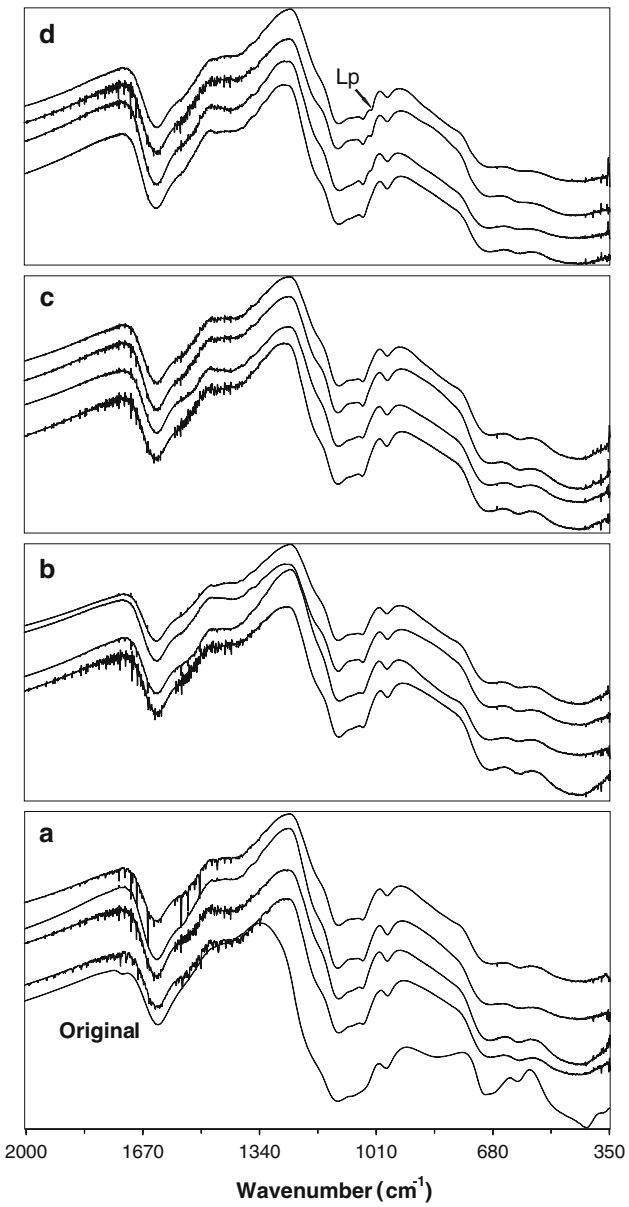

Fig. 4 Fourier transformed IR spectra of the transformed products of SHM and SHM-As at **a** 0.0, **b** 0.4, **c** 0.7, and **d** 1.0 mM $Fe(II)_{aq}$. The original IR spectrum of schwertmannite (SHM) is shown in **a** (*marked as original*). The spectra from *bottom to top* represent transformed products after 5, 58, and 154 h for SHM and 154 h for SHM-As. The *y-axis* represents transmission

Lakind and Stone (1989) demonstrated an increase in deprotonated sites on iron mineral surfaces with increased pH. The alkaline pH used in this study must have developed a negative charge, favoring $FeOH^+$ or $Fe(OH)_2$ surface adsorption and reduced dissolution of STM, which hindered SO_4^{2-} release compared to observations in the absence of $Fe(II)_{aq}$ (0 mM). A closer look into the SO_4^{2-} release profiles (Fig. 6a) clearly showed that aqueous SO_4^{2-} concentrations increased with time, and more release was observed in the presence of 1.0 mM $Fe(II)_{aq}$, compared to 0.4 mM $Fe(II)_{aq}$ from both specimens, indicating that although STM dissolution was reduced in the presence of $Fe(II)_{aq}$ due to rapid adsorption, the higher Fe(II) surface enrichment triggered STM dissolution, causing a slow, enhanced SO_4^{2-} release.

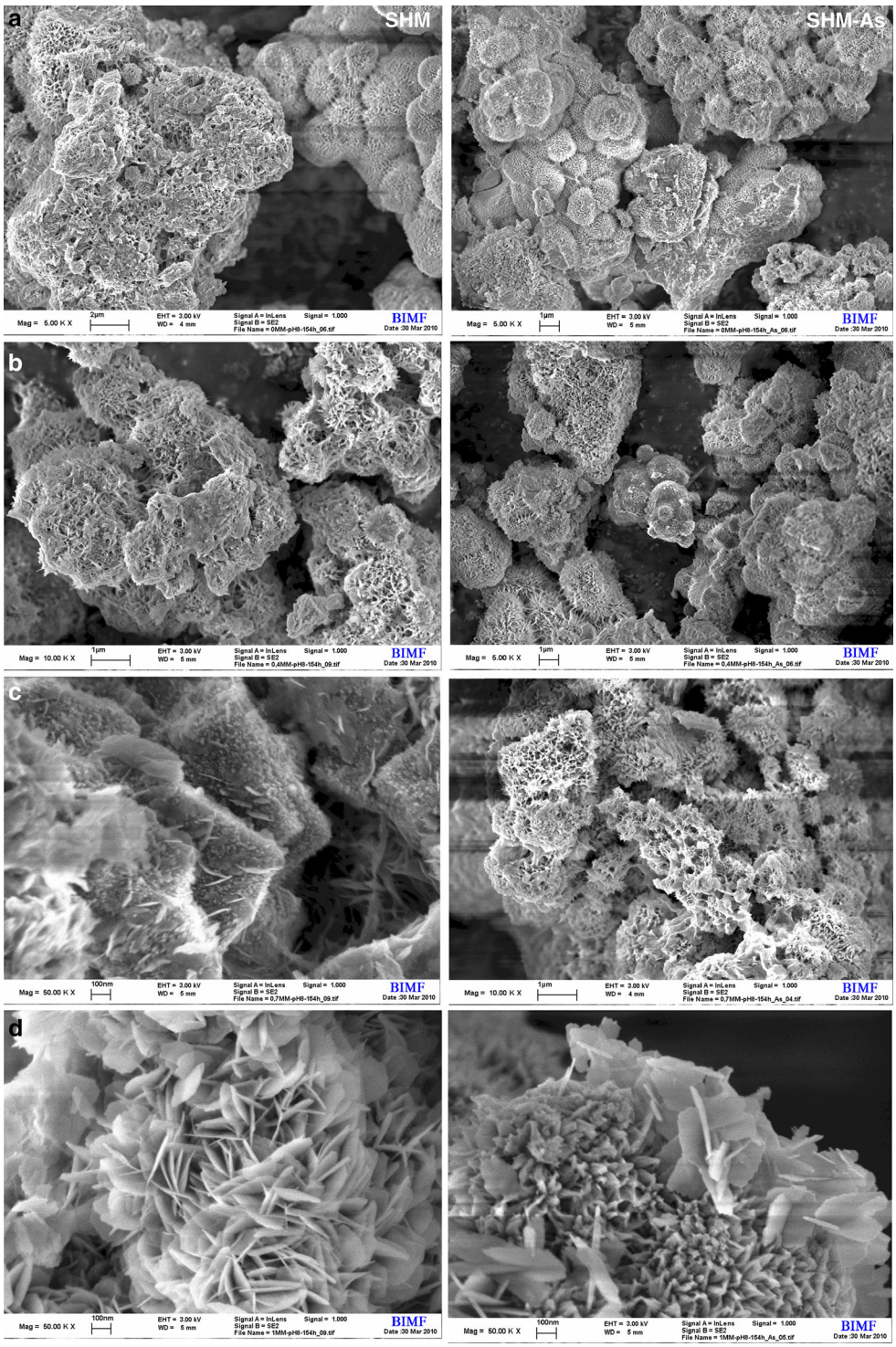

Fig. 5 Scanning electron microscopic images of transformed products of schwertmannite (marked as SHM) and As(III) loaded schwertmannite (*marked as SHM-As*) after 154 h in presence of at 0.0 (**a**), 0.4 (**b**), 0.7 (**c**) and 1.0 mM (**d**) $Fe(II)_{aq}$. The original SEM images before ageing are shown in Fig. 1

Arsenic Mobilization

A fraction of the sorbed As(III) was mobilized during SHM-As transformation; the rate of release was time dependent, with the maximum amount released in the presence of 1.0 mM $Fe(II)_{aq}$ comprising only $\approx$0.02 % ($\approx$21 μg L^{-1}) of the sorbed solid phase fractions (Fig. 6b). Consistent with similar observations during STM to Gt transformation (Acero et al. 2006; Burton et al. 2010), the well-crystallized Lp formation in the presence of 1.0 mM $Fe(II)_{aq}$, compared to that formed with 0.0–0.7 mM $Fe(II)_{aq}$, might have a lower As(III) affinity

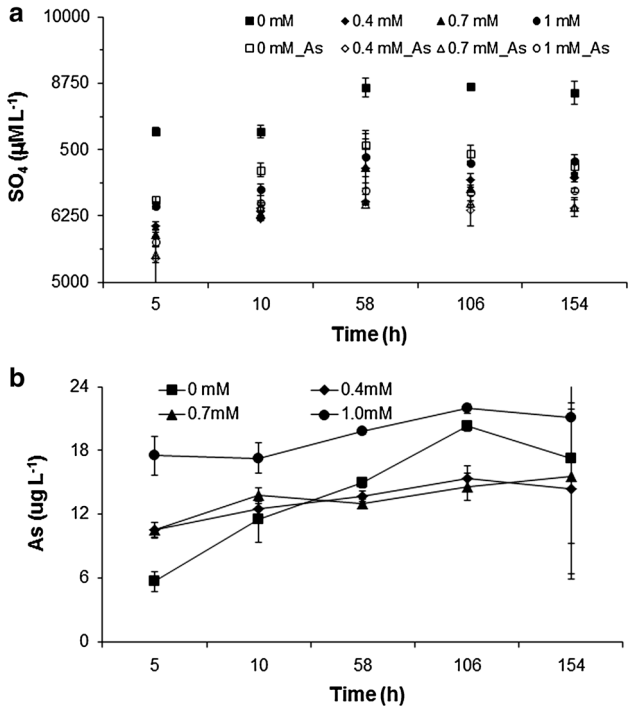

Fig. 6 Plot showing amount of sulphate released at various $Fe(II)_{aq}$ concentrations from **a** schwertmannite and As(III)-loaded schwertmannite and **b** amount of As(T) mobilized from As(III)-loaded schwertmannites (SHM-As)

compared to precursor STM. Also, because STM was also found along with Lp, it is likely that most of the immobilized solid bound As(III) was still incorporated within the STM. More crystalized minerals (e.g. STM vs. Lp) are believed to have lower trace metal retention affinities (Courtin-Normade et al. 2005). Further, Fe(II) adsorption on iron oxide surfaces is believed to increase particle size significantly (Jönsson et al. 2005; Pederson et al. 2005), which might have reduced the sorption capacity of transformed products. Thus, released As(III) during SHM-As dissolution did not readsorb onto Lp due to its poor affinity and/or larger particle size, possibly explaining the higher As(III) release as SHM-As transformed to Lp.

Possible Schwertmannite–Lepidocrocite Transformation Mechanism

Although Gt is reported as a common abundant end product during Fe(II)-catalyzed STM transformation, Lp constituted a minor phase from the previous research (e.g. Burton et al. 2007, 2008) or was even not formed in the presence of 10 mM $Fe(II)_{aq}$ after 9 days (Burton et al. 2010). The formation of Lp is still controversial, as many researchers believe that Lp never forms from ferric species (Jolivet et al. 2006), while others have reported formation from oxidation of Fe(II) (Cornell and Schwertmann 2006).

Previous researchers have demonstrated two possible mechanisms for transformation of poorly crystalline/amorphous iron oxides to well crystalized thermodynamically stable forms, i.e. dissolution/re-precipitation and solid-state transformation. Solid-state transformation commonly occurs when the precursor and transferred product are of identical crystal structure (e.g. Fh–Hm transformation; Andreeva et al. 1995; Cudennec and Lecerf 2006; Liu et al. 2005, 2007a, b; Schwertmann et al. 1999; Yee et al. 2006) and is favored at high temperature conditions (Henderson and Sullivan 2010). Formation of Lp in the current experimental conditions demonstrates that an absolute solid-state transformation might not have occurred because of the different crystal structure of STM (tetragonal) and Lp (orthorhombic) (Cornell and Schwertmann 2006) and the room temperature. However, this process cannot be completely overruled, considering the lower SO_4^{2-} release in the presence of $Fe(II)_{aq}$ compared to that in the absence of $Fe(II)_{aq}$. If Lp formation were happening only due to the dissolution-reprecipitation mechanism, the complete $Fe(II)_{aq}$ adsorption within 5 h should have resulted in elevated SO_4^{2-} concentrations in the $Fe(II)_{aq}$ reactors, since dissolved Fe(II) catalyzes STM dissolution (Burton et al. 2007, 2010). On the other hand, although higher SO_4^{2-} release was observed in the absence of $Fe(II)_{aq}$, indicating better STM dissolution, formation of Lp was not evident from XRD, IR, and SEM observations. Thus, it may be that the rapid adsorption of $Fe(II)_{aq}$ reduced dissolution but facilitated solid-state transformation by electron transfer between adsorbed Fe(II) and the Fe(III) crystal lattice (Jeon et al. 2003; Williams and Scherer 2004). $Fe(III)_{aq}$ was not found in this study. This generally indicates dissolution (Liu et al. 2005, 2007a, b), but while a Fe(III) precipitate could have rapidly formed, the elevated aqueous SO_4^{2-} concentrations clearly demonstrates dissolution. Close observation of aqueous SO_4^{2-} profiles between 0.4 and 1.0 mM (Fig. 6a) demonstrates higher dissolution in the presence of higher $Fe(II)_{aq}$. As Fe(II) surface loading increased at elevated $Fe(II)_{aq}$, it could have led to more electron transfer between Fe(II) and Fe(III), which would have increased dissolution rates significantly (Larsen and Postma 2001; Suter et al. 1991). The complete adsorption of added $Fe(II)_{aq}$ on STM surfaces within 5 h, without any evidence of new phase formation, indicates that adsorbed $Fe(II)_{aq}$ took part in the electron transfer process on the surface, which is considered a slow kinetic process where the electron from the adsorbed Fe(II) transfers into the crystal lattice of STM releasing Fe(III). As the Fe(II)-O bond is more labile than Fe(III)-O bond, the presence of additional electrons on the crystal lattice would have decreased the stability of STM and led to dissolution (Pederson et al. 2005).

A pH close to the pH_{PZC} favors solid state transformation due to low solubility (Liu et al. 2005; Schwertmann et al. 1999). The current experimental pH was slightly higher than the literature-reported pH_{PZC} values ($pH_{PZC} = 6.6$, Regenspurg et al. 2004; $pH_{PZC} = 7.2$, Jönsson et al. 2005), which should favor solid state transformation. Similar to Gt, Lp is generally believed to form by a dissolution-reprecipitation process (Cornell et al. 1989; Schwertmann et al. 1999). As the present experiments were conducted at room temperature (22 ± 2 °C), conditions might not have favored a dehydration reaction causing a solid-state transformation as proposed by Schwertmann et al. (1999) and Liu et al. (2005). Thus, the current observation might be due to both processes having governed the overall transformation, or one predominant controlling process.

$Fe(OH)_2$ is believed to be the predominant species at pH >7.4 (Martell and Smith 1982; Morgan and Lahav 2007), which accelerates solid state transformation, compared to dissolution-reprecipitation on Fe(III) minerals, based on previous studies (Liu et al. 2005). Hence, the two processes might have acted together. In the dissolution-reprecipitation processes, the dissolved Fe(II) might have been rapidly adsorbed on STM, blocking the surface for aggressive dissolution. The adsorbed Fe(II) then might have transfered into the Fe(III) crystal lattice through electron transfer, releasing Fe(II) as $Fe(OH)^{2+}$ or $Fe(OH)_2^+$ into solution, which then precipitated as Lp. In solid-state transformation, the adsorbed Fe(II) favors electron transfer, which accelerates STM transformation, as was clearly observed in the presence of 1.0 mM $Fe(II)_{aq}$, where Lp was formed, compared to what occurred with less or no $Fe(II)_{aq}$.

Conclusions

This study has potential implications for understanding schwertmannite metastability in anoxic alkaline environments. Schwertmannite may undergo morphological degradation at alkaline pH without transformation to any new iron (hydr)oxides in the absence of dissolved ferrous iron, while the presence of at least 700 μM $Fe(II)_{aq}$ can lead to schwertmannite transforming to lepidocrocite within 4 days. Schwertmannite transformed incompletely to lepidocrocite at pH 8. Lepidocrocite formation was accelerated by increased dissolved ferrous iron concentrations, possibly by catalytic effects through schwertmannite dissolution and reprecipitation of lepidocrocite crystallites and/or through solid-state electron transfer between adsorbed Fe(II) and the Fe(III) crystal lattice. Schwertmannite that already contains adsorbed As(III) was found to be relatively resistant to the catalytic effect of $Fe(II)_{aq}$, slowing down lepidocrocite formation.

Acknowledgments This work was supported by the German Academic Exchange Service (DAAD) and the Geotechnologien programme (BMBF, No-03G0714A) and was performed at the University of Bayreuth, Germany. Dr. Janneck (GEOS, Freiburg) provided the schwertmannite sample. We thank the reviewers for their suggestions on how to improve the data presentation.

References

Acero P, Ayora C, Torrento C, Nieto J (2006) The behavior of trace elements during schwertmannite precipitation and subsequent transformation into goethite and jarosite. Geochim Cosmochim Acta 70:4130–4139

Andreeva D, Mitov I, Tabakova T, Mitrov V, Andreev A (1995) Influence of iron (II) on the transformation of ferrihydrite into goethite in acid medium. Mater Chem Phys 41:146–149

Bigham JM, Schwertmann U, Carlson L, Murad E (1990) A poorly crystallized oxyhydroxysulfate of iron formed by bacterial oxidation of Fe(II) in aid mine waters. Geochim Cosmochim Acta 54:2743–2758

Bigham JM, Schwertmann U, Traina SJ, Winland RL, Wolf M (1996) Schwertmannite and the chemical modeling of iron in acid sulfate waters. Geochim Cosmochim Acta 60:2111–2121

Boily J, Gassman PL, Peretyazhko T, Szanyi J, Zachara JM (2010) FTIR spectral components of schwertmannite. Environ Sci Technol 44:1185–1190

Burton ED, Bush RT, Sullivan LA, Mitchell DRG (2007) Reductive transformation of iron and sulfur in schwertmannite rich accumulations associated with acidified coastal lowlands. Geochim Cosmochim Acta 71:4456–4473

Burton ED, Bush RT, Sullivan LA, Mitchell DRG (2008) Schwertmannite transformation to goethite via the Fe(II) pathway: reaction rates and implications for iron–sulfide formation. Geochim Cosmochim Acta 72:4551–4564

Burton ED, Johnston SG, Watling K, Bush RT, Keene AF, Sullivan LA (2010) Arsenic effects and behavior in association with the Fe(II)-catalyzed transformation of schwertmannite. Environ Sci Technol 44:2016–2021

Carlson L, Bigham JM, Schwertmann U (2002) Scavenging of As from acid mine drainage by schwertmannite and ferrihydrite: a comparison with synthetic analogues. Environ Sci Technol 36:1712–1719

Collins RN, Jones AM, Waite TD (2010) Schwertmannite stability in acidified coastal environments. Geochim Cosmochim Acta 74:482–496

Cornell RM, Schwertmann U (2006) The iron oxides, structure, properties, reactions, occurences and uses. Wiley-VCH Gmbh & Co., Weinheim

Cornell RM, Schneider W, Giovanoli R (1989) Phase transformations in the ferrihydrite/cysteine system. Polyhed 8:2829–2836

Courtin-Normade A, Grosbois C, Bril H, Roussel C (2005) Spatial variability of arsenic in some iron-rich deposits generated by acid mine drainage. Appl Geochem 20:383–396

Cudennec Y, Lecerf A (2006) The transformation of ferrihydrite into goethite or hematite, revisited. J Solid State Chem 179:716–722

Davidson LE, Shaw S, Benning LG (2008) The kinetics and mechanism of schwertmannite transformation to goethite and hematite under alkaline conditions. Am Mineral 93:1326–1337

Egal M, Casiot C, Morin G, Parmentier M, Bruneel O, Lebrun S, Elbaz-Poulichet F (2009) Kinetic control on the formation of tooeleite, schwertmannite and jarosite by *Acidithiobacillus ferrooxidans* strains in an As(III)-rich acid mine water. Chem Geol 265:432–441

Fukushi K, Sasaki M, Sato T, Yanase N, Amano H, Ikeda H (2003) A natural attenuation of arsenic in drainage from an abandoned arsenic mine dump. Appl Geochem 18:1267–1278

Glombitza F, Janneck E, Arnold I, Rolland W, Uhlmann W (2007) Eisenhydroxisulfate aus der Bergbauwasserbehandlung als Rohstoff. Heft 110 der Schriftenreihe der GDMB, S, pp 31–40, ISBN 3-935797-35-4

Henderson SP, Sullivan LA (2010) Low temperature transformation of schwertmannite to hematite with associated CO_2, SO and SO_2 evolution. In: Proceedings of 19th world congress of soil science, soil solutions for a changing world, pp 72–75

Jeon B, Dempsey BA, Burgos WD (2003) Kinetics and mechanisms for reactions of Fe(II) with iron(III) oxides. Environ Sci Technol 37:3309–3315

Johnston SG, Keene AF, Burton ED, Bush RT, Sullivan LA (2011) Iron and arsenic cycling in intertidal surface sediments during wetland remediation. Environ Sci Technol 45:2179–2185

Jolivet J, Tronc E, Chanéac C (2006) Iron oxides: from molecular clusters to solid; a nice example of chemical versatility. Comptes Rendus Geosci 338:488–497

Jönsson J, Persson P, Sjöberg S, Lovgren L (2005) Schwertmannite precipitated from acid mine drainage: phase transformation, sulfate release and surface properties. Appl Geochem 20:179–191

Knorr K, Blodau C (2007) Controls on schwertmannite transformation rates and products. Appl Geochem 22:2006–2015

Kumpulainen S, Räisänen ML, Von der Kammer F, Hofmann T (2008) Ageing of synthetic and natural schwertmannites at pH 2–8. Clay Min 43:437–448

LaKind JS, Stone AT (1989) Reductive dissolution of goethite by phenolic reductants. Geochim Cosmochim Acta 53:961–971

Larsen O, Postma D (2001) Kinetics of reductive bulk dissolution of lepidocrocite, ferrihydrite, and goethite. Geochim Cosmochim Acta 65:1367–1379

Liu H, Wei Y, Sun Y (2005) The formation of hematite from ferrihydrite using Fe(II) as a catalyst. J Mol Catal A Chem 226:135–140

Liu H, Wei Y, Li P, Zhang Y, Sun Y (2007a) Catalytic synthesis of nanosized hematite particles in solution. Mater Chem Phys 102:1–6

Liu H, Li P, Zhu M, Wei Y, Sun Y (2007b) Fe(II)-induced transformation from ferrihydrite to lepidocrocite and goethite. J Solid State Chem 180:2121–2128

Liu H, Guo H, Li P, Wei Y (2009) Transformation from δ-FeOOH to hematite in the presence of trace Fe(II). J Phys Chem Solid 70:186–191

Martell E, Smith RM (1982) Critical stability constants. Plenum Press, New York

McArthur JM, Ravenscroft P, Safiullah S, Thirlwall MF (2001) Arsenic in groundwater: testing pollution mechanisms for sedimentary aquifers in Bangladesh. Water Resour Res 37:109–117

Morgan B, Lahav O (2007) The effect of pH on the kinetics of spontaneous Fe(II) oxidation by O_2 in aqueous solution—basic principles and a simple heuristic description. Chemosphere 68:2080–2084

Morin G, Juillot F, Casiot C, Bruneel O, Personné J, Elbaz-Poulichet F, Leblang M, Ildefonse P, Calas G (2003) Bacterial formation of tooeleite and mixed arsenic(III) or arsenic(V)-iron(III) gels in the Carnoule's acid mine drainage, France. A XANES, XRD, and SEM study. Environ Sci Technol 37:1705–1712

Paikaray S, Peiffer S (2010) Dissolution kinetics of sulfate from schwertmannite under variable pH conditions. Mine Water Environ 29:263–269

Paikaray S, Peiffer S (2012) Abiotic schwertmannite transformation kinetics and the role of sorbed As(III). Appl Geochem 27:590–597

Paikaray S, Göttlicher J, Peiffer S (2011) Removal of As(III) from acidic waters using schwertmannite: surface speciation and effect of synthesis pathway. Chem Geol 283:134–142

Paikaray S, Göttlicher J, Peiffer S (2012) As(III) retention kinetics, equilibrium and redox stability on biosynthesized schwertmannite and its fate and control on schwertmannite stability on acidic (pH 3.0) aqueous exposure. Chemosphere 86:557–564

Paikaray S, Essilfie-Dughan J, Göttlicher J, Pollok K, Peiffer S (2014) Redox stability of As(III) on schwertmannite surfaces. J Hazard Mater 265:208–216

Pederson HD, Postma D, Jakobsen R, Larsen O (2005) Fast transformation of iron oxyhydroxides by the catalytic action of aqueous Fe(II). Geochim Cosmochim Acta 69:3967–3977

Pederson HD, Postma D, Jakobsen R (2006) Release of arsenic associated with the reduction and transformation of iron oxides. Geochim Cosmochim Acta 70:4116–4129

Peretyazhko T, Zachara JM, Boily JF, Xia Y, Gassman PL, Arey BW, Burgos WD (2009) Mineralogical transformations controlling acid mine drainage chemistry. Chem Geol 262:169–178

Regenspurg S, Brand A, Peiffer S (2004) Formation and stability of schwertmannite in acidic mining lakes. Geochim Cosmochim Acta 68:1185–1197

Schroth AW, Parnell RA (2005) Trace metal retention through the schwertmannite to goethite transformation as observed in a field setting, Alta Mine, MT. Appl Geochem 20:907–917

Schwertmann U, Carlson L (2005) The pH-dependent transformation of schwertmannite to goethite at 25°C. Clay Miner 40:63–66

Schwertmann U, Friedl J, Stanjek H (1999) From Fe(III) ions to ferrihydrite and then to hematite. J Colloid Interface Sci 209:215–223

Suter D, Banwart S, Stumm W (1991) Dissolution of hydrous iron(III) oxides by reductive mechanisms. Langmuir 7:809–813

Tabatabai MA (1974) A rapid method for determination of sulfate in water samples. Environ Lett 7:237–243

Tamura H, Goto K, Yotsuyanagi T, Nagayama G (1974) Spectrophotometric determination of iron(II) with 1, 10-phenanthroline in the presence of large amounts of iron(III). Talanta 21:314–318

Wang H, Bigham JM, Tuovinen OH (2006) Formation of schwertmannite and its transformation to jarosite in the presence of acidophilic iron-oxidizing microorganisms. Mater Sci Eng C 26:588–592

Webster JG, Swedlund PJ, Webster KS (1998) Trace metal adsorption onto an acid mine drainage iron (III) oxy hydroxy sulfate. Environ Sci Technol 32:1361–1368

Williams AGB, Scherer MM (2004) Spectroscopic eviden:ce for Fe(II)–Fe(III) electron transfer at the Fe oxide–water interface. Environ Sci Technol 38:4782–4790

Winland RL, Traina SJ, Bigham JM (1991) Chemical composition of ochreous precipitates from Ohio coal mine drainage. J Environ Qual 20:452–460

Yee N, Shaw S, Benning LG, Nguyen TH (2006) The rate of ferrihydrite transformation to goethite via the Fe(II) pathway. Am Miner 91:92–96